Theor Chem Acc (1997) 96:84–91

Theoretical
Chemistry Accounts

A case against large cluster-induced nonequilibrium solvent effects in supercritical water

Huaqiang Luo, Susan C. Tucker

Department of Chemistry, University of California, Davis, CA 95616, USA

Received: 8 January 1997 / Accepted: 17 January 1997

Abstract. Using a partially compressible continuum solvation model, we have shown that solvent compression in just the first two solvation shells (or thereabouts) is all that is required to gain the bulk of the compression-induced enhancement to the solvation energy of ions in supercritical water. This result is found to hold even when the direct, equilibrium solvent-solute cluster involves well over a hundred solvent molecules. We argue that, for charge variation reactions in supercritical water, the observed short-range behavior of the compression-induced solvation free energy precludes the existence of any anomalously large nonequilibrium solvent effects which might be expected on the basis of the very large size of the equilibrium clusters.

Key words: Solvent effects – Supercritical water – Free energy of solvation – Continuum electrostatics

1 Introduction

It has been well established that solvent-solute clustering plays an important role in the energetics of solvation in supercritical fluids (SCFs) in their compressible regimes [1–15]. It has also been demonstrated that for reactive solutes in such dilute SCF solutions the degree of solvent clustering under equilibrium conditions can be strongly reaction-path dependent [3, 4, 16]. We therefore ask whether nonequilibrium solvent effects associated with reaction-path-dependent solvent clustering should be expected in SCFs. In this work we explore the effects of solvent compression on solvation in order to shed light on this question.

In general, the effect of a solvent on a solute's reaction rate can be broken down into two components: the equilibrium and the nonequilibrium solvent effects [17–21]. The equilibrium effects arise when the solute's solvation free energy varies along the reaction path, causing the solution-phase reaction free energy profile to differ from that in the gas phase. However, if the equilibrium solvent configuration varies substantially along the solute reaction path, the associated solvent reorganizational motion must occur on the time scale of the solute reaction if the aforementioned equilibrium picture is to be valid. When, instead, the solvent reorganization is very slow, this reorganization process may slow down or even control the solute reaction, and such effects are known as nonequilibrium solvent effects.

Extensive effort has been directed towards finding and understanding such nonequilibrium solvent effects on solute reactions [17–21]. In particular, it was expected that large nonequilibrium effects would be observed for charge transfer or charge separation reactions in aqueous solution, as a result of the slow rotational reorientation time for water. It turns out, however, that the dipolar rearrangement of the solvent necessitated by such charge redistribution in the solute can be largely accomplished through small librational motions of water molecules in the first solvation shell. As a result, the time scale associated with the requisite solvent rearrangements is much faster than expected, and the observed nonequilibrium effects were correspondingly less important than expected [22].

The discovery of reaction-path-dependent solvent clustering in dilute SCFs raises a similar question about whether we should expect large nonequilibrium solvent effects associated with this phenomena. On the one hand, very large solvent clusters are known to form around solutes under equilibrium conditions in SCFs, and the formation of such large clusters, which requires the collective motion of many solvent molecules (see below), is expected to be a very slow process. Consequently, quite large nonequilibrium effects might be expected for reactions in which such clusters need to be formed as the reaction proceeds in order to provide equilibrium solvation of the products. Yet, as was the case in ambient aqueous solution, this slow time scale event will only give rise to a large nonequilibrium effect if the full motion is required for reaction. That is, if the full cluster must be created to effectively solvate the products, nonequilibrium effects would be expected to

Correspondence to: S. Tucker

be unusually large, but if the bulk of the solvation energy can be attained via some smaller, less time-consuming process – such as density enhancement in just the first one or two solvation shells – then no unusually large nonequilibrium effects would be expected.

Herein we examine the cluster- (or compression-) induced enhancement of the solvation energy of a charged solute in supercritical water (SCW). In particular, we determine the degree to which the full equilibrium cluster must be formed or, more precisely, the range over which such clustering must occur, for this enhancement in the solvation energy to be obtained.

2 Background

In dilute SCFs, there are two distinct solvent-solute clustering, or density-enhancement, effects, and it is necessary to be explicit about which of these behaviors, if not both, are being considered or probed in a given calculation or experiment [23–30]. The distinction between these two effects has been most clearly given by Chialvo and Cummings [23], who showed that, for an infinitely dilute solute in an SCF solvent, the partial molar volume – which measures the solvent-solute density enhancement – can be decomposed into a sum of two components corresponding to the two effects.

The first, or indirect, component is proportional to $\kappa_T c_{12}$, where κ_T is the SCFs isothermal compressibility and c_{12} is the direct solvent-solute correlation function. This indirect component, then, diverges as does the compressibility when the critical point of the SCF is approached from above, reflecting the critical behavior of the pure solvent. It is this indirect, divergent component which is responsible for the extremely large partial molar volumes observed in SCFs near their critical points. While such partial molar volumes indicate that the indirect solvent compression effect involves hundreds of molecules, it has already been shown that this 'critical condensation' does not contribute to the solute's free energy of solvation, which itself depends only on the direct correlation function, and not on the diverging compressibility [23,25,26]. The insensitivity of the solvation energy to the indirect compression effect reflects the fact that these effects, i.e. the correlated long-range, near-critical density fluctuations of the solvent, occur outside of the range of the solute-solvent interaction potential and thus do not alter the energetics. It follows that such fluctuations will not generate nonequilibrium solvent effects on reacting solutes, and, as such, we do not consider this indirect component of the solvent density enhancement further.

The second, or direct, component of the partial molar volume is proportional to just the direct solvent-solute correlation function c_{12}, and, as such, it remains finite as the critical point is approached and the SCFs correlation length diverges [23]. This direct component reflects solvent-solute clustering which arises as a direct result of an attractive solvent-solute interaction potential and extends only over the range of this potential. Note that the direct effect is frequently termed the 'short-range effect,' because its range remains finite as the critical point of the SCF solvent is approached, in contrast to the divergent range of the indirect effect. However, when the solute-solvent interactions involve long-range coulombic forces, the range of the direct, 'short-range' compression effect can, in fact, be quite large (although still finite). As we shall show by example below, the number of solvent molecules involved in such direct compression effects can be well over a hundred. We therefore examine the question of whether large, direct solvent-solute clusters are likely to give rise to nonequilibrium solvent effects. We do so by determining the range over which direct compression effects contribute substantially to the solvation energy.

There have been two previous studies in which the range dependence of thermodynamic quantities related to the solvation free energy was examined in SCFs [25,26]. Although neither of these works examine the particular question of interest herein, that is, over what range the *direct compression* contributes to these solvation quantities, the conclusions therein are of some interest. Munoz and Chimowitz [25] considered the residual chemical potential of a Lennard-Jones solute, μ_r, in a supercritical Lennard-Jones fluid. Using that this chemical potential can be cast as an integral over all space, i.e. $\mu_r = \int_0^\infty f_{12}(r)\, d\mathbf{r}$, these authors found that the partially integrated quantity $\int_0^R f_{12}(r)\, d\mathbf{r}$ attains 90% of the full value of the chemical potential μ_r within a range of about two solvation shells. This 'short-range' behavior of the residual solute chemical potential arises directly from the short-range nature of the Lennard-Jones solvent-solute interaction potential, as can be seen because the r-dependence of the integrand $f_{12}(r)$ is determined by an overlap of the radial distribution function [31] with the intermolecular potential function and thus does not exceed the range of this potential. Unfortunately, the authors did not separate out the compression-induced part of the chemical potential; nor did they consider the range of the direct component of the density enhancement. We are thus unable to assess the range over which compression affects the chemical potential; however, the observed result of two solvation shells clearly provides an outer bound to this range.

Tom and Debenedetti [26] considered the range dependence of the solute fugacity coefficient, also for a supercritical Lennard-Jones solute-solvent system. These authors found results similar to those of Munoz and Chimowitz, in that partial integration of the fugacity-coefficient integrand demonstrated that 98% of the value of the fugacity coefficient is attained within about three solvation shells, again establishing an outer bound on the region in which compression may be important. While these authors did look at the range dependence of the solvent density enhancement, they did not separate out the nondivergent, direct component of this enhancement in which we are interested. Thus, both of these studies demonstrate that short-range properties determine solvation. Yet, both studies considered only short-range, Lennard-Jones interaction potentials. As such, they provide no predictions regarding the range behavior of the solvation properties when long-range coulombic interactions are involved. In particular, they

leave completely open the question of the range over which direct compression will alter the solvation.

3 Methods

We use a completely compressible (CC) continuum electrostatic model, described elsewhere [4,32], to represent a charged solute/SCW system. From this model we can extract both the structureless equilibrium solvent density distribution around the solute, $\rho(\mathbf{r})$, and the equilibrium Gibbs free energy of solvation ΔG_{CC} [3]. The compression-induced part of this solvation energy, ΔG_{c}, is found by comparing the solvation energy evaluated from the CC model, ΔG_{CC}, with that evaluated from an incompressible (IC) continuum electrostatic model [33,34], ΔG_{IC}, i.e. $\Delta G_{\mathrm{c}} \equiv \Delta G_{\mathrm{CC}} - \Delta G_{\mathrm{IC}}$. In order to elucidate the range over which solvent compression plays an instrumental role in generating the compression-induced component of the solvation free energy, ΔG_{c}, we introduce a partially compressible (PC) continuum solvation model as described below.

In the IC model, the solute is represented by a set of point charges in a vacuum cavity defined by interlocking atomic spheres, and the solvent is represented as a dielectric medium characterized by a dielectric constant ϵ_{IC} everywhere outside of the solute cavity. The CC model differs from the IC model only in that the dielectric 'constant' of the fluid outside of the solute cavity, $\epsilon_{\mathrm{CC}}(\mathbf{r})$, is allowed to vary locally according to the solvent density enhancements (solvent compression) induced by the solute-generated electric field. Note that the final electric field in the CC case, E_{CC}, will differ from that in the IC case, E_{IC}, because in the CC case the final field E_{CC} must be self-consistent with the field-dependent dielectric constant, $\epsilon_{\mathrm{CC}}(E_{\mathrm{CC}}(\mathbf{r}))$. In the PC model, solvent compression, and thus a locally varying dielectric 'constant,' is allowed only in a shell of thickness a around each of the interlocking spheres defining the solute cavity. In the cases studied herein, all of the atomic spheres have the same radii, r_{c}, and thus the size of the compressible shell is denoted by the outer radius of the shell, $R = r_{\mathrm{c}} + a$. Note that since the region outside of the compressible shell is treated as an incompressible medium with dielectric constant ϵ_{IC}, the PC model reduces to the IC model limit when $R = r_{\mathrm{c}}$ and to the CC model limit when $R \to \infty$.

The compression-induced solvation energy in the PC model depends upon the radius of the compressible shell, that is, $\Delta G_{\mathrm{c}}(R) = G_{\mathrm{PC}}(R) - G_{\mathrm{IC}}$, and has the limiting values $\Delta G_{\mathrm{c}}(R = r_{\mathrm{c}}) = 0$ and $\Delta G_{\mathrm{c}}(R \to \infty) = \Delta G_{\mathrm{c}}$ for the CC model. The reader should keep in mind that, in contrast to earlier studies [25,26], this R-dependence represents successive, complete calculations of the total solvation energy with differing ranges of allowed compression, and *not* simply the distance dependence of the integrated free energy density in a single CC calculation. These two quantities are in general not equivalent, because in the CC case, compression outside of the shell R can alter the electric field, and thus the energy density, within the shell. Additionally, the size of the compressible shell alters the value of the field in the IC region outside of the shell. As a result, the integrated energy density from a single CC calculation would not represent the case of partial compression in which we are interested (and which is represented by the PC model).

In addition to the compression-induced solvation energy, we consider the excess number of solvent molecules around the solute, defined as

$$N_x = \int_{r_{\mathrm{c}}}^{\infty} [\rho_x(\mathbf{r}) - \rho_{\mathrm{b}}] \mathrm{d}\mathbf{r} \tag{1}$$

where ρ_{b} is the bulk density, and $\rho_x(\mathbf{r})$ is the equilibrium solvent density distribution evaluated with solvent model x, where x is IC, CC or PC(R), and R denotes the outer radius of the compressible shell. Again, $N_{\mathrm{PC}}(R = r_{\mathrm{c}}) = 0$, which is the IC result, $N_{\mathrm{PC}}(R \to \infty) = N_{\mathrm{CC}}$, which is the excess number in the CC model, and the R-dependence represents successive, complete calculations of the total excess number when different ranges of compression are allowed.

The basic equations for the free energies and densities are presented briefly below [3,4,32,35–37], as these relations will aid in the interpretation of the results. The electrostatic work, and thus the free energy, of charging a solute in the presence of a dielectric fluid is given by the sum of the work required to create the final field in vacuo plus the work done on the fluid during the charging process. The final field, E_x, where x denotes the IC, CC or PC(R) model, is given by the solution of Poisson's equation with self-consistent values for the field-dependent local dielectric constant $\epsilon_x(E_x\mathbf{r})$, within the constraints of model x. The free energy of charging the solute in the presence of a model x solvent is then written in terms of the final field E_x as [3,4,32,35]

$$G_x = \int \frac{1}{2}\epsilon_0 E_x^2 \mathrm{d}\mathbf{r} + \int w_{e,x}\, \mathrm{d}\mathbf{r}. \tag{2}$$

Note that the solvation energy for model x is simply $\Delta G_x = G_x - G_0$, where G_0 is the work of charging the solute in a vacuum.

The second term in Eq. (2) is a sum over the work, $w_{e,x}$, done on each volume element of the fluid outside of the solute cavity. This work is given by [32,35]

$$w_{e,\,x}(\mathbf{r}) = \int_0^{E_x(\mathbf{r})} \epsilon_0 E' \mathrm{d}[(\epsilon_x(E') - 1)E'] \ , \tag{3}$$

where the dependence of the local dielectric constant on the local field is shown explicitly. In the IC case, ϵ_{IC} is a constant, and this work term reduces to the familiar result,

$$w_{e,\mathrm{IC}} = \frac{1}{2}\epsilon_0(\epsilon_{\mathrm{IC}} - 1)E_{\mathrm{IC}}^2 \ . \tag{4}$$

Finally, in the CC and PC models, the local density $\rho_x(\mathbf{r})$ is determined by the local field $E_x(\mathbf{r})$ according to integration of the expression [3,37]

$$\mathrm{d}\rho_x = \frac{1}{2}\epsilon_0 \rho_x^2 \kappa_T \left(\frac{\partial \epsilon}{\partial \rho}\right)_{E_x,T} \mathrm{d}(E_x^2) \tag{5}$$

where the compressibility and the density dependence of the dielectric constant are found as described elsewhere [3]. This latter relation also allows direct evaluation of $\epsilon_x(\mathbf{r})$ from $\rho_x(\mathbf{r})$.

4 Models

We consider two simple model solutes, a monatomic ion represented by a single unit point charge in a cavity of radius $r_c = 2$ Å, and a diatomic ion represented by two half-unit partial charges in a cavity defined by two overlapping spheres of radii $r_c = 2$ Å separated by a distance 4 Å. In both cases the cavity dielectric constant is taken to be 1. Note that for the monatomic ion, the CC and PC models were solved using the method of Wood et al. [32, 35]. For the diatomic ion, these models were solved using the numerical grid treatment of Luo and Tucker [4] for the solute plus solvent system out to a radius of 8 Å. Boundary conditions for this inner grid were determined by self-consistent compressible continuum calculations for the outer solvent sphere, which were computed using the method of Wood et al. [32, 35].

The solvation of these model ions at the three SCW sate points listed in Table 1 was considered. States A and B were chosen to have the same bulk dielectric constant but different compressibilities, with state A being the more compressible state. State C has a lower density and a lower bulk dielectric constant than either state A or state B, and is even less compressible that state B.

5 Results and discussion

5.1 CC model

The CC continuum solvation model is used to compute the equilibrium solvent density distribution, which is structureless in the present model, around each of the monatomic and diatomic ion solutes for each of the three SCW states described above. The excess number of water molecules around the solute is in each case computed from the corresponding density distribution via Eq. (1), and these excess numbers are shown in Table 2. Considering the monatomic ion, one sees that, as expected, N_{CC} increases dramatically with increasing solvent compressibility, having values of 15, 18 and 126, for reduced compressibilities of 1.34, 1.92 and 14.7 for states C, B and A, respectively.

Comparing the numbers of molecules involved in the solvent compression for the monatomic and diatomic solutes, one finds that N_{CC} is smaller for the diatomic ion under all conditions. This result is expected, because the electric field generated by two partial charges is everywhere smaller than that due to a single point charge, thus leading to less electrostriction. Notice, however, that the decrease in N_{CC} between the two solute models is much greater for the more compressible state A, for which N_{CC} drops from 126 to 64, than for states B and C, which drop from 18 to 16 and 15 to 12, respectively. That N_{CC} is so dramatically different for these two solvent models in SCW at state A reflects the sensitivity of the local solvent density to small variations in the electric field that arises from the very large compressibility of this state.

The equilibrium free energy of solvation in the CC model, ΔG_{CC}, is the solvation energy that would be achieved if the solvent were allowed to reorganize – i.e. compress – to its equilibrium density distribution. These solvation energies are shown along with the solvation energies computed assuming no compression, ΔG_{IC} (Eqs. 2 and 4), in Table 2. Notice first that the IC model solvation free energies are the same for states A and B, because these states have the same bulk dielectric constant, $\epsilon_{IC} = 4.1$. The magnitude of the IC solvation energies for state C, which has $\epsilon_{IC} = 2.24$, is correspondingly smaller. When complete compression is allowed, the solvation becomes more favorable, such that the magnitude of ΔG_{CC} exceeds that of ΔG_{IC} in all cases. The extra, compression-induced solvation energies, ΔG_c, are also given in Table 2.

Comparison of ΔG_c for states A and B yields the expected result that the compression effect on the solvation energy is greater for the more compressible state A, consistent with the larger N_{CC} values observed for this state. However, the compression effects on the free energy of the least compressible state C are noticeably larger than those for states A and B. This somewhat puzzling result arises because the dependence of the solvation energy on the dielectric constant of the solvent is highly nonlinear, as exemplified by the factor $(1 - (1/\epsilon))$ in the Born expression for the solvation energy of a point charge. Thus, if compression were to change the effective dielectric constant from 2 to 3, this prefactor, and thus the magnitude of ΔG, would increase by a factor of 4/3, whereas if the change in the dielectric constant were from 4 to 5, the magnitude of ΔG would increase only by a factor of 16/15. Consequently, if two states of different bulk dielectric constant, such as states B and C, show similar compression, and thus a similar change in the bulk dielectric constant (because the density dependence of the dielectric constant is fairly linear) [38], the state with the lower initial dielectric constant will yield a greater compression-induced stabilization of the solute. In the case of states A and C, this non-linear dielectric

Table 1. SCW states studied[a]

State	P (MPa)	T (K)	ρ(g cm^{-3})	T/T_c	ρ/ρ_c	ϵ	κ_T/κ_T^{IG}[b]
A	23.4	653.0	0.250	1.01	0.77	4.11	14.7
B	44.3	740.0	0.275	1.14	0.85	4.11	1.92
C	45.8	841.1	0.162	1.30	0.50	2.24	1.34

[a] All quantities from Ref. [39] except ϵ from Ref. [38]
[b] κ_T^{IG} is the compressibility of an ideal gas under the same thermodynamic conditions

Table 2. Free energies of solvation (in kcal/mol)

State	Monatomic				Diatomic			
	ΔG_{IC}	ΔG_{CC}	ΔG_c	N_{CC}	ΔG_{IC}	ΔG_{CC}	ΔG_c	N_{CC}
A	−62.8	−74.2	−11.4	126	−47.3	−54.3	−7.1	64
B	−62.8	−71.6	−8.8	18	−47.3	−53.7	−6.5	16
C	−45.9	−62.6	−16.7	15	−34.4	−44.4	−10.1	12

effect on ΔG is sufficient to counteract, and in fact exceed, the effect of the much greater compression which occurs in state A. Lastly, note that for each of the three states, ΔG_c is of smaller magnitude for the diatomic ion than for the monatomic ion, consistent with the reduced field and lesser compression of the former model. Again, the change in ΔG_c between the two models is largest at state C, as a result of the nonlinear dependence of the solvation energies on the dielectric constant.

5.2 PC model

5.2.1 Compressible-range dependence

The PC continuum model, PC(R), is used to compute the solvation free energy $\Delta G_{PC}(R)$ (Eq. 2) and solvent density distribution, summarized by the excess number of solvent molecules $N_{PC}(R)$ (Eq. 1), for a solvent which may compress out to distances R away from the solute center, but which is incompressible beyond this range. The PC model thus mimics a short-time, nonequilibrium situation in which only nearby solvent molecules have had the opportunity to readjust to a newly created solute charge distribution. We ask, then, what percent of the complete, equilibrium compression-induced solvation energy, ΔG_c, is achieved through such partial compression. Towards this end, we consider the compressible-range-dependent quantity,

$$\text{Rel } \Delta G_c(R) = \frac{\Delta G_{PC}(R) - \Delta G_{IC}}{\Delta G_{PC}(R \to \infty) - \Delta G_{IC}}, \tag{6}$$

which is zero in the IC limit ($R = r_c$) and one in the CC limit ($R \to \infty$). Note that the denominator is simply ΔG_c for the CC model. The compressible-range dependence of the relative compression-induced stabilization, Rel $\Delta G_c(R)$, is shown in Fig. 1a for all three SCW states for the monatomic ion solute; results for the diatomic ion solute are qualitatively similar and are therefore not shown. For comparison, we show in Fig. 1b the compressible-range dependence of the compression, or rather, of the relative number of excess molecules,

$$\text{Rel } N(R) = \frac{N_{PC}(R)}{N_{PC}(R \to \infty)}, \tag{7}$$

which becomes zero in the IC limit, because $N_{IC} = 0$, and one in the CC limit. The diatomic ion results are again qualitatively similar to the monatomic ion results which are shown.

From Fig. 1 a and b it is immediately evident that the compressible-range required to attain the bulk of the compression-induced solvation energy is much shorter than that required to attain complete compression, i.e. to attain the CC value for N. Said another way, we find that a small fraction of the complete equilibrium compression contributes the bulk of the complete compression-induced solvation energy. For example, for state A, values of Rel $N(R = 6\,\text{Å}) = 0.12$ and Rel $\Delta G_c(R = 6\,\text{Å}) = 0.83$ mean that $N_{PC}(R = 6\,\text{Å}) = 15$ of the complete $N_{CC} = 126$ excess water molecules will yield 83%, or −9.5 kcal/mol, of the complete compression-induced

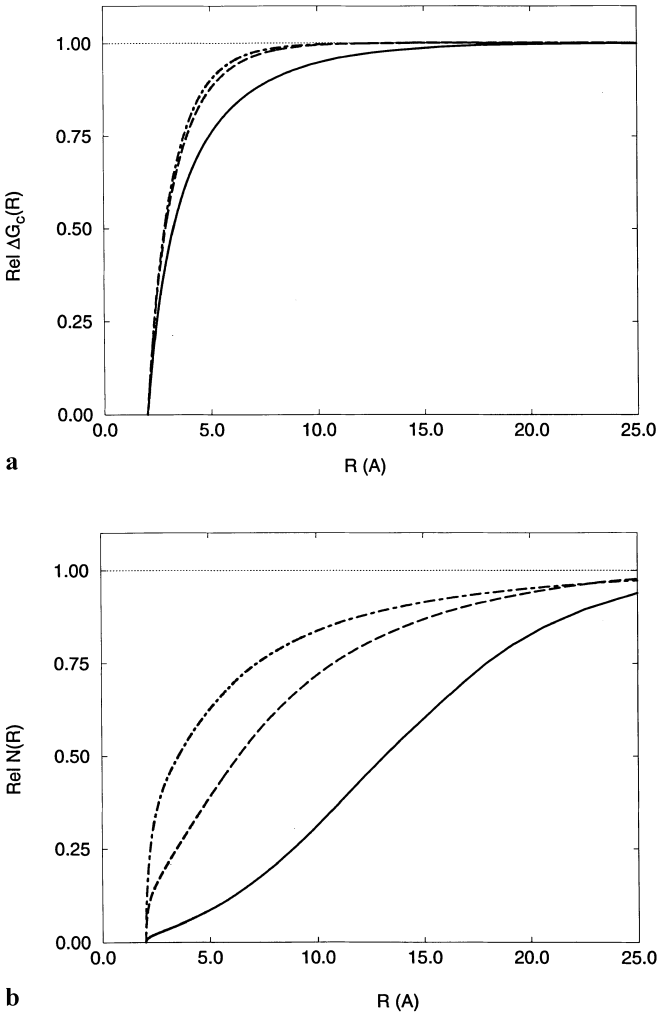

Fig. 1a,b. The range-dependence of **a** the relative compression-induced component of the solvation free energy and **b** the relative excess number of molecules for states A (*solid*), B (*dashed*) and C (*dot-dashed*)

solvation energy of $\Delta G_c = -11.4$ kcal/mol. Note that the bulk density of SCW in state A is only 0.25 g cm^{-3} and that even with the addition of 15 water molecules to the 6Å shell, the local density remains below the liquid density of 1.0 g cm^{-3}.

Comparison of the compressible-range dependences of the three SCW states shows that, while the range over which compression contributes to ΔG_c increases for increasingly compressible SCW states, this range increases much more slowly than does the range over which compression occurs, which increases dramatically. This increase is illustrated by SCW state A, for which the range of compression exceeds the 25 Å shown. This is in contrast with the compression-induced solvation energy, which is dominated by first and second solvation shell effects for all three SCW states considered. That is, if compression is allowed only in a 4 Å shell around the solute ($R = 6\,\text{Å}$) – a region corresponding roughly to the range of the first two solvation shells of water – 83%, 93% and 95% of the complete compression-induced solvation energy ΔG_c is achieved in SCW states A, B and

C, respectively. First solvation shell effects alone account for 65%, 79% and 80% of the complete ΔG_c, despite representing only 6%, 30% and 55% of the complete number of excess water molecules, respectively. We conclude that even though the size of the equilibrium, direct solvent-solute clusters may grow dramatically with solvent compressibility, the effect of this compression on the solvation energetics will be controlled by the compression of a relatively small number of solvent molecules in the first few solvation shells. As a result, it is expected that for charge variation reactions in SCW, equilibrium solvation along the reaction path can be accomplished through local solvent compression in the first few solvation shells, and, therefore, that anomalously large solvent effects associated with a need to form extremely large solvent clusters as the reaction proceeds will not be observed.

5.2.2 Short-ranged nature of ΔG_c

In this section we show, qualitatively, that the very different compressible-range (R) dependences observed for the relative compression-induced solvation energy, Rel $\Delta G_c(R)$, and the relative excess number of solvent molecules, Rel $N(r)$, arise as a result of significant differences in the electric field dependences of these quantities. To begin, we recognize that the changes which occur in Rel $\Delta G_c(R)$ and Rel $N(R)$ when additional compression is allowed in the region between R and $R + \delta R$ arise primarily from contributions to these quantities from the newly compressed region, because there was no contribution from this region when it was incompressible. A secondary contribution arises because the additional compression can change the electric field over the entire fluid, thus altering the contributions of other volume elements of the fluid. If we ignore this secondary effect, the compressible-range (R) dependences of ΔG_{PC} and N_{PC} in Eqs. (6) and (7) become simply the radial dependence (r) in the CC model, of the contribution of each volume element to the total quantities ΔG_c and N_{CC}. The problem is thus reduced to determining the r-dependence of the compression-induced solvation-energy-density, Δg_c, and of the solvent density, ρ. Note that the r-dependence of both Δg_c and ρ originates from their dependence on the local electric field $E(r)$, and it is therefore instructive to consider the electric-field dependences of these quantities, i.e. $\Delta g_c(E_{CC}(r))$ and $\rho(E_{CC}(r))$. In what follows, we make this comparison for the case of the monatomic ion.

The field dependence of the solvent density in the CC model, $\rho(E_{CC})$, where E_{CC} is the local field in this model, is given by integration of Eq. (5) from zero to E_{CC}. Note that the maximum field strength considered for each SCW state is the value attained at the solute cavity boundary. The field-dependent densities for the monatomic ion in SCW states A and B are shown in Fig. 2a. One sees that $\rho(E_{CC})$ are highly nonlinear functions characterized by a rapid rise in density. The field strength at which this rapid rise in density occurs is seen to depend upon the compressibility of the SCW state, occurring at weaker field for the more compressible state.

The E-field dependence of the compression-induced component of the solvation free energy density, $\Delta g_c(r) = g_{CC}(r) - g_{IC}(r)$, where $g_x(r)$ is the appropriate integrand of Eq. (2), must be considered in comparison. Explicitly,

$$\Delta g_c = \frac{1}{2}\epsilon_0 E_{CC}^2 + w_{e,CC}(E_{CC}) - \frac{1}{2}\epsilon_0 E_{IC}^2 - w_{e,IC}(E_{IC}), \quad (8)$$

where E_{CC} and E_{IC} are the E-fields at r in the CC and IC models, respectively. In order to compare the energy density to the solvent density (Fig. 1a), Δg_c must be written in terms of the field variable for the CC model, E_{CC}. In general, the field at **r** in the IC model can be related to the field at **r** in the CC model by some function $\gamma(\mathbf{r})$, such that

$$E_{IC}(\mathbf{r}) = \gamma(\mathbf{r}) E_{CC}(\mathbf{r}). \quad (9)$$

For the specific case of a point charge, the function $\gamma(\mathbf{r})$ depends only on the local field at **r**, such that Eq. (9) becomes simply

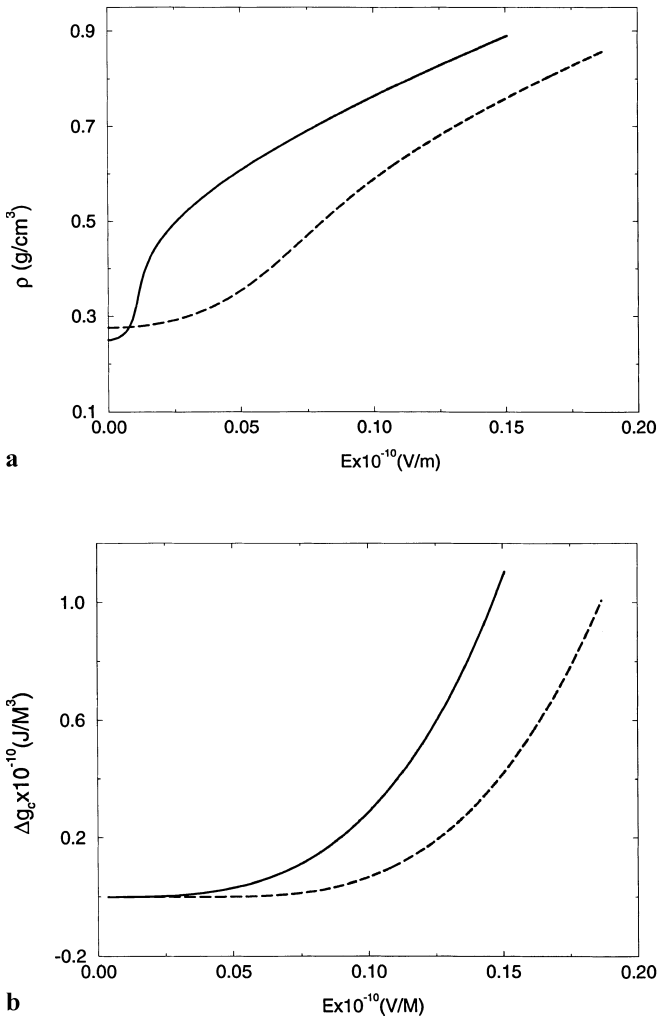

Fig. 2a,b. The E-field dependence of **a** the solvent density and **b** the compression-induced solvation energy density for states A (*solid*) and B (*dashed*)

$$E_{IC} = \gamma(E_{CC})E_{CC} \tag{10}$$

where

$$\gamma(E_{CC}) = \frac{\epsilon_{CC}(E_{CC})}{\epsilon_{IC}} \ . \tag{11}$$

As a result, the field dependence of the energy density becomes (with Eq. 4)

$$\Delta g_c = \frac{1}{2}\epsilon_0 E_{CC}^2 + w_{e,CC}(E_{CC}) - \frac{1}{2}\epsilon_0 \epsilon_{IC} \gamma^2 E_{CC}^2. \tag{12}$$

By realizing that $w_{e,CC}$ can be approximately described by an equation of the form of Eq. (4) with an effective dielectric constant, one can see that, within a scaling factor, all terms in Δg_c go as $\mathcal{O}(E_{CC}^2)$, which is a very different field dependence than that exhibited by the solvent density $\rho(E_{CC})$.

In Fig. 2b, $\Delta g_c(E_{CC})$ is shown for comparison with $\rho(E_{CC})$ in Fig. 2a. Clearly the compression-induced solvation energy density falls off rapidly with decreasing field strength. In contrast the solvent density remains substantially enhanced to much lower field strengths, particularly for the most compressible state A. Consequently, in regions very near the solute where field strengths are strong, there is substantial compression ($\rho(E_{CC}) > \rho_b$), and this compression has a noticeable effect on the solvation free energy density ($\Delta g_c \neq 0$). Away from the solute, weak fields may still cause substantial compression ($\rho(E_{CC}) > \rho_b$), but this compression has little effect on the free energy density ($\Delta g_c \approx 0$). Comparison of SCW states A and B shows that this effect is magnified as the compressibility increases and even weaker fields are able to induce density enhancements. And, because the electric field falls off with distance only as $\mathcal{O}(r^{-2})$, the spatial range over which the density enhancement is important but the free-energy density enhancement is not can be quite large, as was observed in Fig. 1.

Finally, $\rho(E_{CC})$ and $\Delta g_c(E_{CC})$ for the monatomic ion in SCW state C are shown in Fig. 3. Note that for this case the nonlinear behavior of $\rho(E_{CC})$ occurs at sufficiently high field strengths that it noticeably alters the quadratic behavior of $\Delta g_c(E_{CC})$ through its effect on $\gamma(E_{CC})$ and $w_{e,CC}(E_{CC})$. This contrasts with the results for SCW states A and B, in which rapid changes in $\rho(E_{CC})$ occur at smaller fields and thus do not noticeably alter the behavior of $\Delta g_c(E_{CC})$. Additionally, this late rise in $\rho(E_{CC})$ means that large field strengths are required to cause compression, as well as to alter the solvation energy density. Thus, as the compressibility of the fluid decreases, the range over which there is substantial compression shrinks down towards the range over which the compression-induced solvation energy density is affected.

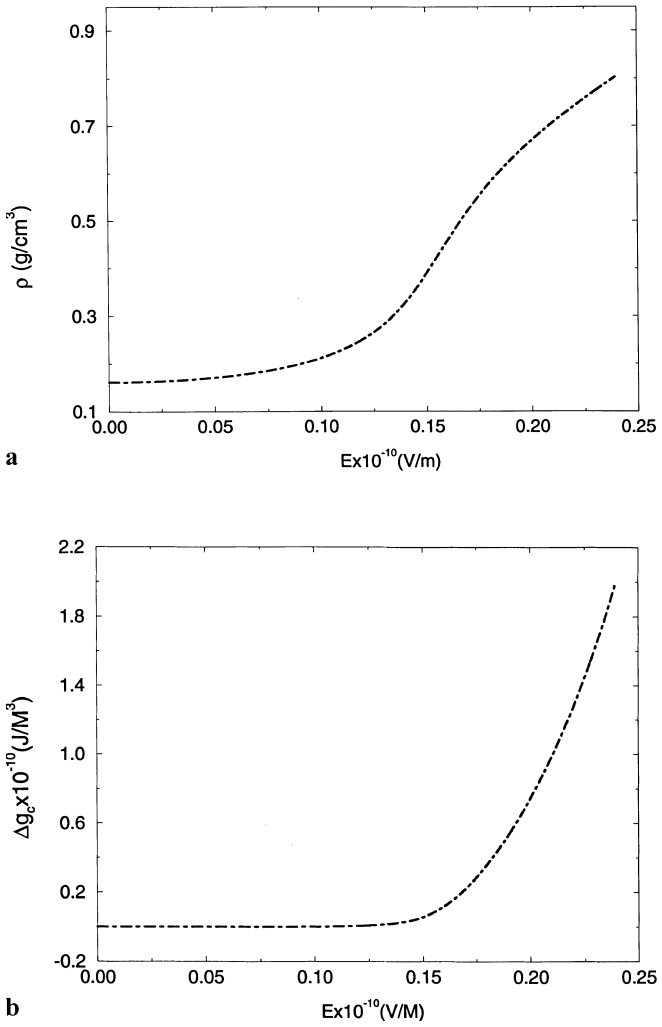

Fig. 3a,b. Same as Fig. 2, except for state C

6 Conclusions

A partially compressible continuum solvation model was used to explore the compressible-range dependence of the compression-induced solvation free energy for model ions in SCW under various conditions. It was found that the range over which solvent compression affects the solvation free energy can be substantially smaller than the range of the compression itself. This result follows from the fact that, for highly compressible solvents, weak fields far from the solute ion can induce substantial solvent density enhancements, whereas the stronger fields close to the solute ion are required to enhance significantly the solvation energy density, which grows in only as the field squared. In fact, for all cases considered, the compression-induced solvation free energy is largely determined by compression within the first two solvation shells. Thus, in spite of the very large numbers of solvent molecules which may be involved in the equilibrium, direct solvent-solute clusters (often called 'short-range' density enhancement effects), only a small number of these molecules are actually required to achieve near equilibrium-solvation energetics. We therefore conclude that anomalously large nonequilibrium solvation effects, which might be expected on the basis of the very large size of the equilibrium clusters, are not likely to occur in charge-variation reactions in SCW.

Acknowledgements. This material is based on work supported by the National Science Foundation under grant no. CHE-9307679. S.C.T. gratefully acknowledges an NSF Young Investigator Award and a Camille Dreyfus Teacher-Scholar Award.

References

1. Savage P E, Gopalan S, Mizan T I, Martino C J, Brock E E (1995) AIChE J 41:1723
2. Brennecke J F (1993) In: Kipran E, Brennecke J F (eds) Supercritical fluid engineering science. ACS Symposium Series. ACS, Washington, DC
3. Luo H, Tucker S C (in press) J Phys Chem
4. Luo H, Tucker S C (1996) J Phys Chem 100:11165
5. Luo H, Tucker S C (1995) J Am Chem Soc 45:11359
6. Tucker S C, Gibbons E M (1994) In: Truhlar D G, Cramer C J (eds) Structure and reactivity in aqueous solution. ACS Symposium Series. ACS, Washington, DC
7. Johnston K P, Bennett G E, Balbuena P B, Rossky P J (1996) J Am Chem Soc 118:6746
8. Bennett G E, Rossky P J, Johnston K (1995) J Phys Chem 99:16136
9. Flanagin L W, Balbuena P B, Johnston K P, Rossky P J (1995) J Phys Chem 99:5196
10. Cummings P T, Chialvo A A, Cochran H D (1994) Chem Eng Sci 49:2735
11. Cummings P T, Cochran H D, Simonson J M, Mesmer R E, Karaborni S (1991) J Chem Phys 94:5606
12. Urdahl R S, Rector K D, Meyers D J, Davis P H, Fayer M D (1996) J Chem Phys 105:8973
13. Gupta R B, Johnston K P (1994) Ind Eng Chem Res 33: 2819
14. Sun Y P, Fox M A, Johnston K P (1992) J Am Chem Soc 114:1187
15. Johnston K P, Haynes C (1987) AIChE J 33:2017
16. Balbuena P B, Johnston K P, Rossky P J (1995) J Phys Chem 99:5196;(1994) J Am Chem Soc 116:2689
17. Voth G A, Hochstrasser R M (1996) J Phys Chem 100:13034
18. Tucker S C (1995) In: Talkner P, Hänggi P (eds) New trends in Kramers reaction rate theory, understanding chemical reactivity. Kluwer, Dordrecht
19. Hynes J T (1993) Chem Phys 176:521
20. Hänggi P, Talkner P, Borkovec M (1990) Rev Mod Phys 62:250
21. Hynes J T (1985) In: Baer M (ed) Theory of chemical reaction dynamics CRC Press, Boca Raton, p 171
22. This is a simplified picture; see Ref. [17], Section X, for a more complete picture
23. Chialvo A A, Cummings P T (1994) AIChE J 40:1558
24. Carlier C, Randolph T W (1993) AIChE J 39:876
25. Munoz F, Chimowitz E H (1992) Fluid Phase Eq 71:237
26. Tom J W, Debenedetti P G (1993) Ind Eng Chem Res 32:2118
27. Wu R -S, Lee L L, Cochran H D (1992) J Supercrit Fluids 5:192
28. Knutson B L, Tomasko D L, Eckert C A, Debenedetti P G, Chialvo A A (1992) In: Bright F V, McNally M E (eds) ACS Symposium Series 488, ACS, Washington, DC
29. Mcguigan D B, Monson P A (1990) Fluid Phase Eq 57:227
30. Debenedetti P G (1987) Chem Eng Sci 42:2203
31. Technically, it is the pair correlation function with the system coupled to extent ξ, where ξ is the Kirkwood coupling parameter, which is involved in the overlap integral
32. Wood R H, Quint J R, Grolier J -P E (1984) J Phys Chem 85:3944
33. Gilson M, Sharp K A, Honig B (1988) J Comp Chem 9:327
34. Cramer C J, Truhlar D G (1995) In: Boyd D B, Lipkowitz K B (eds) Reviews in computational chemistry. VCH, New York
35. Wood R H, Carter R W, Quint J R, Majer V, Thompson P T, Boccio J O (1994) J Chem Thermodyn 26:225
36. Wood R H, Quint J R (1989) J Phys Chem 93:936
37. Frank H S (1955) J Chem Phys 23:2023
38. Archer D G, Wang P (1990) J Phys Chem Ref Data 19:371
39. Hill P G (1990) J Chem Phys Ref Data 19:1233